Towards quantitative symmetry energy constraints from isospin transport in heavy ion collisions

C Ciampi, S Mallik, F Gulminelli, D Gruyer, J D Frankland, N Le Neindre, R Bougault, A Chbihi

Towards quantitative symmetry energy constraints from isospin transport in heavy ion collisions

C. Ciampi,[1,*] S. Mallik,[2,3,†] F. Gulminelli,[4] D. Gruyer,[4]
J. D. Frankland,[1] N. Le Neindre,[4] R. Bougault,[4] and A. Chbihi[1]

[1] *Grand Accélérateur National d'Ions Lourds (GANIL), CEA/DRF–CNRS/IN2P3, Boulevard Henri Becquerel, F-14076 Caen, France*
[2] *Physics Group, Variable Energy Cyclotron Centre, 1/AF Bidhan Nagar, Kolkata 700064, India*
[3] *Homi Bhabha National Institute, Training School Complex, Anushakti Nagar, Mumbai 400085, India*
[4] *Université de Caen Normandie, ENSICAEN, CNRS/IN2P3, LPC Caen UMR6534, F-14000 Caen, France*

Heavy ion reactions provide a unique opportunity to measure the Equation of State (EoS) of baryonic matter in a large density domain, but to get quantitative constraints observables have to be used that are as insensitive as possible to final state interaction, and at the same time robustly predicted by transport models with limited model dependence. In this work, we compare for the first time BUU transport calculations to the impact parameter dependence of the isospin transport ratio deduced from INDRA-FAZIA data [1]. Using different state-of-the-art nuclear functionals, provided both by *ab initio* calculations and by phenomenological approaches, a confidence region for the symmetry energy is extracted, which can be used to inform Bayesian inference of the neutron star EoS.

Heavy-ion collisions (HIC) are unique probes to explore in the laboratory nuclear matter in density conditions different from the one of ground state atomic nuclei, and can thus potentially bring constraints to the nuclear Equation of State (EoS) [2], an essential ingredient to the interpretation of gravitational wave data, see Ref. [3] and references therein. This is particularly true in the (ultra)relativistic regime [4], where collective flows and particle production can be confronted with transport model calculations in controlled numerical settings [5, 6] to extract the density dependence of the symmetry energy [7] in a density domain lying between the one explored by *ab initio* calculations [8] and nuclear structure experiments [9, 10], and the one probed by astrophysical measurements [11]. Still, the HIC intermediate energy domain provides complementary observables that can meaningfully enrich the available constraints, with the additional advantage that the momentum dependence can still be controlled by the effective mass formalism, and uncertainties on the elementary reaction rates are strongly reduced.

In particular, the differential transfer of protons and neutrons between projectile and target, dubbed isospin diffusion, can be measured by the Isospin Transport Ratio (ITR), defined as [12]:

$$R(x) = \frac{2x_i - x_{(A+A)} - x_{(B+B)}}{x_{(A+A)} - x_{(B+B)}}. \qquad (1)$$

Here x is an isospin sensitive observable extracted from the final state of reactions between two nuclides A and B, with different neutron-richness, with $i = (A+B), (B+A)$. The value x_i measured for reactions between nuclei with different neutron content is normalized to the reference values obtained when the same nuclide is used for both projectile and target, $(A + A)$ and $(B + B)$. The pioneering works of the MSU group [13] showed that the ITR is strongly correlated to the density dependence of the symmetry energy, allowing the exclusion of extreme values for its magnitude and slope around saturation density ($E_{\rm sym}$ and $L_{\rm sym}$ parameters) [14]. However, to get quantitative constraints different delicate points need to be addressed: (1) the isospin sensitive observable must be chosen such that it is directly measurable and at the same time robustly predicted by the transport model [15]; (2) the reaction centrality assessment must be reliable and readily comparable between model and data; (3) the density range probed by the ITR in the studied reactions must be estimated to avoid uncontrolled extrapolations.

In this paper, we propose significative improvements to all these points. First, the ITR is evaluated using the directly measured neutron to proton ratio of the quasiprojectile remnant [1, 16], a particularly robust observable for the transport models, providing an ITR with very limited sensitivity to secondary decay [17]. This key improvement was possible due to the excellent isotopic identification performance of the FAZIA apparatus [18, 19], able to achieve mass discrimination for heavy nuclei up to $Z \approx 25$. Second, for the centrality assessment we employ a model-independent method to reconstruct the impact parameter distributions contributing to each data point [20]. Finally, we employ state-of-the-art functionals [21] for the model comparison and estimate precisely the density associated to the isospin transfer by correlating the time evolution of the isospin current densities [22] and the nuclear density.

We consider ^{58,64}Ni+^{58,64}Ni reactions at 32 MeV/nucleon measured with the INDRA-FAZIA apparatus: this dataset has been employed also in Refs. [16, 23], where further experimental details can be found. The experimental data has been analyzed [1] with the aim of producing the most model-independent results possible in order to facilitate comparison with

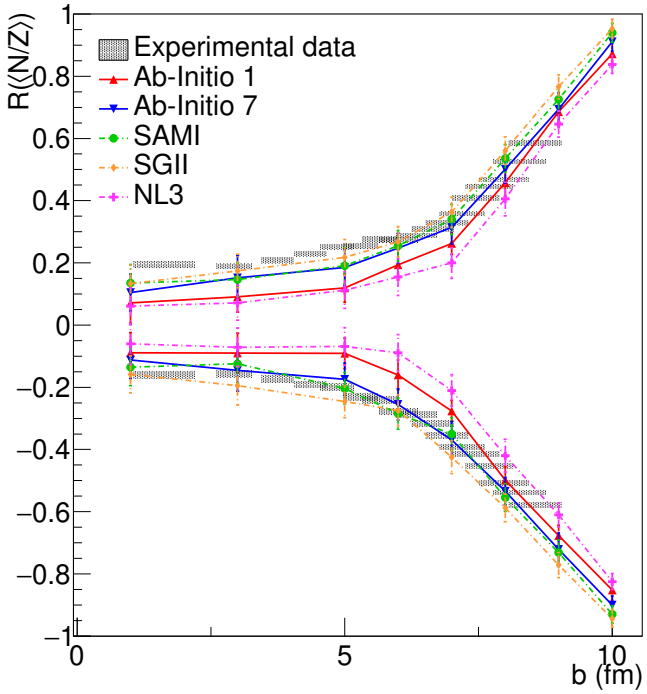

FIG. 1: Impact parameter dependence of the isospin transport ratio R obtained from the average neutron to proton ratio $\langle N/Z\rangle$ of quasiprojectile for ^{64}Ni+^{58}Ni and ^{58}Ni+^{64}Ni reactions at 32 MeV/nucleon. The experimental results from Ref. [1], represented with the shaded gray rectangles, are compared with BUU@VECC-McGill model calculations adopting *ab initio* 1 (red upward triangles), *ab initio* 7 (blue downward triangles), SAMI (green circles), SGII (orange diamonds) and NL3 (magenta crosses) EoS parametrizations. Lines are drawn to guide the eyes.

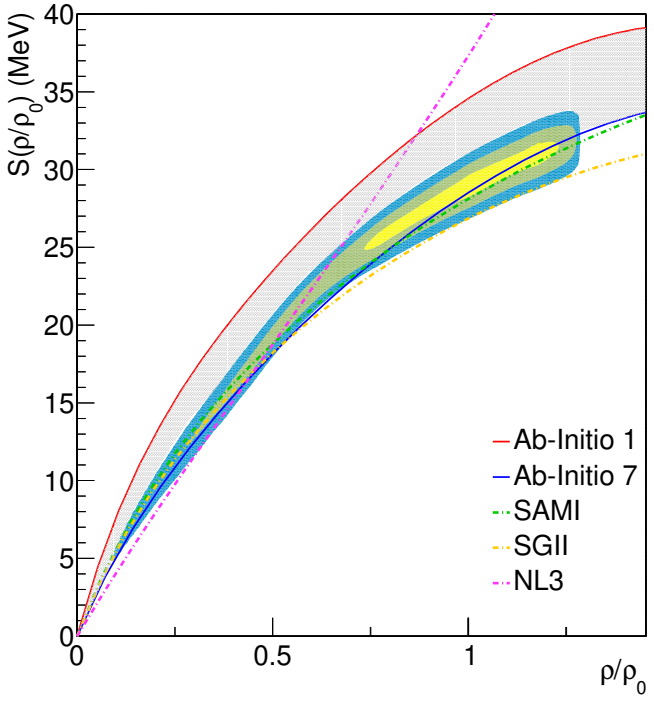

FIG. 2: Density dependence of symmetry energy from *ab initio* 1 (red), *ab initio* 7 (blue), SAMI (green), SGII (orange) and NL3 (magenta) EoS. Dash-dotted lines indicate phenomenological models, while solid lined indicate those obtained from *ab initio* approaches. The gray band indicates the uncertainty on the chiral constraint. The constraint obtained from this work is represented by the regions in yellow, green and blue corresponding to 1σ, 2σ, 3σ confidence levels respectively.

the predictions of any transport model. The isospin sensitive observable used to compute the ITR is the average neutron-to-proton ratio $\langle N/Z\rangle$ of the quasiprojectile remnant, identified event-by-event as the forward-emitted fragment with the largest atomic number. The experimental result for the ITR $R(\langle N/Z\rangle)$ as a function of the impact parameter b is plotted in Fig. 1 with shaded rectangles [1], reporting statistical errors on the y-axis, and the combined effect of statistical errors with those associated with the uncertainties in the b reconstruction procedure [20] along the x-axis.

The theoretical calculations are performed using the BUU@VECC-McGill transport model [24, 25], shown to produce results consistent with similar models in the systematic survey conducted by the Transport Model Evaluation Project (TMEP) [5], both for mean-field [26] and nucleon-nucleon collisions [27]. Ground states of the projectile and target nuclei are constructed with a variational method [28] using Myers density profiles [29]. We use 100 test particles per nucleon, and for each reaction at each impact parameter 200 events are simulated. The bulk part of the mean-field is calculated from a meta-functional [21] based on a polynomial expansion in density around saturation and including momentum dependence and deviations from the parabolic isospin dependence through the effective mass and its splitting. To cover the present chiral uncertainty on the density dependence of the symmetry energy at sub-saturation, EoS from two extreme χ-EFT interactions (specifically models 1 and 7 in Ref. [30], here abbreviated as *ab initio* 1 and *ab initio* 7, respectively), are considered. The density dependence of symmetry energy from these two EoS is presented in Fig. 2 with solid lines. The gray band of Fig.2 thus indicates the present uncertainty on the density dependence of the symmetry energy from nuclear matter *ab initio* calculations [30], and the present challenge from HIC observables is to confirm and possibly reduce this uncertainty band.

Since the chiral perturbation theory becomes less controlled starting from densities of the order of the

saturation density ρ_0, we also consider two popular effective models, the relativistic mean-field NL3 [31] and the SGII Skyrme interaction [32], that respect the chiral constraint at low density but correspond to a stiff (respectively, soft) extrapolation for super-saturation matter. Such relatively extreme behaviors were suggested by analyses of neutron skin measurements [33] and pion production data [34], respectively. The symmetry energy density dependence corresponding to these phenomenological approaches is plotted in Fig. 2 with dash-dotted lines. Finally, the Skyrme interaction SAMI [35] is also considered, that corresponds to a symmetry energy behavior almost indistinguishable from *ab initio* 7 but a quite different (and more realistic) behavior for symmetric matter. The comparison between these two models, SAMI and *ab initio* 7, will therefore allow to verify that the adopted observable is indeed suitable to explore symmetry energy properties and is not sensitive to isoscalar ones. For treating finite nuclei, the bulk part is supplemented by a finite range term optimized on nuclear masses [36] as well as Coulomb potential. For more details, we refer the reader to [37].

The ITR predicted by the BUU@VECC-McGill calculations assuming the aforementioned interaction models are displayed in Fig. 1, where the same color scheme as in Fig. 2 is employed. In each case, the calculations are run until convergence of the ITR (see Ref. [17]), and the $\langle N/Z \rangle$ of the primary quasiprojectile, without secondary de-excitation, is considered to evaluate the ITR, thus avoiding possible spurious effects arising from coupling the transport model with an afterburner. The model error bars represent statistical errors due to the finite number of events. The different models here employed fall within the relatively tight limits for the symmetry energy estimated from present constraints (see Fig. 2) and therefore produce similar ITR values, with a similar impact parameter dependence. In particular, we note that the excellent agreement between the *ab initio* 7 and the SAMI results shows that the ITR is indeed probing the density dependence of the symmetry energy.

Figure 1 also allows to compare the experimental ITR to those predicted by the BUU code. It should be noted that such a comparison is possible thanks to the fact that the ITR strongly suppresses systematic effects in the data such as secondary decay [17, 38]. For reference, χ^2 values resulting from the comparison between experimental data and model predictions for the different EoS here considered are reported in Tab. I. Even if the differences among the theoretical predictions are small, we can still see that the models with the highest symmetry energy around saturation, namely NL3 and *ab initio* 1, can be excluded. Interestingly, this appears to be linked to the absolute value of the symmetry energy above $\approx 0.5\rho_0$, more than to the slope parameter: this already suggests that the collision is probing a density interval close to ρ_0. A global agreement is indeed found among the calculations for SAMI, SGII and *ab initio* 7, all characterized by similar symmetry energy values in this density region: as already evident from Fig. 1 and quantitatively expressed by the χ^2 values reported in Tab. I, the results for these three parametrizations are those providing the most satisfying match of the ITR with the experimental data.

The extracted χ^2 values for the parametrizations under test can be employed to provide approximate confidence regions in the $S - \rho/\rho_0$ plane. To do this, we plotted the χ^2 value for each functional as a function of the corresponding value of $S(\rho/\rho_0)$, for different values of ρ/ρ_0. A parabolic dependence of $\chi^2(S(\rho/\rho_0))$ is observed around its minimum and can be extracted by means of a quadratic fit; the result for NL3, giving the worst agreement with the experimental data, has been excluded from the fit procedure. Assuming Gaussian errors, we can express the corresponding likelihood function as $\mathcal{L}(S(\rho/\rho_0)) = \mathcal{L}_{\max}(S(\rho/\rho_0)) \exp(-\chi^2(S(\rho/\rho_0))/2)$, which in turn allows to extract the confidence intervals for $S(\rho/\rho_0)$ for various $N\sigma$ confidence levels.

However, the process of isospin diffusion probes the different densities explored by the system with varying sensitivity, which must be accounted for in view of providing a constraint on the symmetry energy density dependence. To this end, further information on the dynamics of this process can be extracted from the BUU@VECC-McGill transport model calculations, in order to define a weight function $w(\rho/\rho_0)$ quantifying the relative influence of each explored density on the observed final isospin equilibration.

We therefore focus on the baryonic density and on the isospin current density. Their time evolution has been extracted and averaged over 200 events for four different impact parameter settings, namely $b = 3$, 5, 7 and 9 fm, assuming an *ab initio* 7 EoS (similar behaviors are obtained for the SAMI EoS). The behavior for intermediate impact parameters has been obtained through interpolation. At each timestep, the baryonic density is calculated within a spherical volume V of radius $r = 3$ fm around

	χ^2	χ^2/ν	χ^2 (b=3-9 fm)
Ab Initio 1	80.9	2.38	71.2
Ab Initio 7	8.82	0.26	6.77
SAMI	9.38	0.28	7.36
SGII	15.7	0.46	14.6
NL3	118.1	3.47	104.8

TABLE I: χ^2 values obtained by comparing the experimental data with the BUU@VECC-McGill model calculation assuming the five different EoS parametrizations tested in the present work. The first two columns report the values obtained employing all experimental data points, while in the last column only the centrality range between 3 and 9 fm is considered.

the origin of the centre of mass frame; its time evolution is shown in Fig. 3(a) for ^{64}Ni+^{58}Ni at 32 MeV/nucleon for a few impact parameters. The isospin current density is defined as:

$$\vec{j}_I = \Delta\vec{j}_n - \Delta\vec{j}_p, \tag{2}$$

where $\Delta\vec{j}_q = \vec{j}_q^{(P)} + \vec{j}_q^{(T)}$ is the net current density associated to species $q = n, p$ leading to particle exchange from the two colliding nuclei, with:

$$\vec{j}_q^{(X)} = \frac{1}{V}\int_V d^3r \rho_q^{(X)}(\vec{r})\vec{v}_q^{(X)}(\vec{r}). \tag{3}$$

where the local current density is averaged over the same spherical volume V of radius $r = 3$ fm employed for the baryonic density estimation. Here, the local particle density ρ_q^X and velocity $\vec{v}_q^{(X)}$ is calculated by considering separately the test particles belonging to the projectile (P) and target (T) nucleus before the collision. To better follow the dynamics of isospin transfer, the current densities are calculated in the time-dependent principal axis frame, by diagonalizing at each time step the momentum of inertia tensor constructed from test particle positions. The component of the isospin current density along the principal axis is the one contributing to the nucleon exchange between the two colliding nuclei: its time evolution for a few impact parameters is reported in Fig. 3(b) for ^{64}Ni+^{58}Ni at 32 MeV/nucleon, where the positive sign indicates a net neutron flow from projectile to target leading to isospin equilibration, as expected.

In order to build the weight function $w(\rho/\rho_0)$, we note that the role of each explored density on the final phenomenon depends both on the amount of time spent by the system in that condition, and on the isospin current developing at the same time. Therefore, for a given impact parameter, a partial weight function is extracted by cumulating the baryonic density $\rho(t)/\rho_0$ over time, weighted by the corresponding $j_{\rm p.a.}(t)$ as follows:

$$w_b(\rho/\rho_0) = \int_{t_{\rm start}}^{t_{\rm stop}} j_{\rm p.a.}(t)\,\delta(\rho/\rho_0 - \rho(t)/\rho_0)\,dt \tag{4}$$

In this work, we integrate between $t_{\rm start} = 0$ fm/c, corresponding to an initial distance between the projectile and target centers equal to 12 fm, and $t_{\rm stop} = 80$ fm/c, when there is no further contribution of $j_{\rm p.a.}$ (see Fig. 3(b)).

To take into account different impact parameters, we integrate the partial weight functions normalized by their integral over the density $\tilde{w}_b(\rho/\rho_0)$ over the selected b-interval:

$$w(\rho/\rho_0) = \int_{b_{\rm min}}^{b_{\rm max}} \tilde{w}_b(\rho/\rho_0)\,db \tag{5}$$

Here, we consider impact parameters between 3 fm and 9 fm, where most of the information from the experimental data is concentrated. The likelihood function

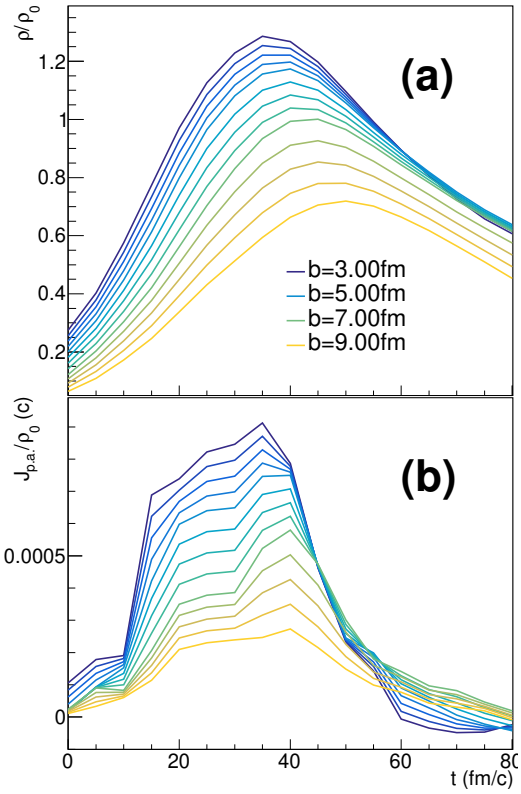

FIG. 3: Time dependence of (a) the baryonic density ρ/ρ_0, (b) the component of the isospin current density along the principal axis $j_{\rm p.a.}/\rho_0$ for ^{64}Ni+^{58}Ni at 32 MeV/nucleon at different impact parameters between b= 3 fm and 9 fm, obtained from BUU@VECC-McGill calculations with *ab initio* 7 EoS.

$\mathcal{L}(S(\rho/\rho_0))$, derived as explained above from the χ^2 values calculated using the experimental ITR data points within this centrality range, is weighted by $w(\rho/\rho_0)$ evaluated over the same interval. Finally, our constraint for the symmetry energy behavior is shown by means of 1σ (yellow), 2σ (green), 3σ (blue) contours in Fig. 2. Our results are in good agreement with the *ab initio* calculations from Refs. [30, 39] but provide tighter constraints in the probed density region. Remarkably, the fact that the densities to which the isospin diffusion is most sensitive remain quite close to saturation density allows us to reject stiff behaviors like the one of the NL3 model, behaviors that could not have been discriminated with data probing only densities below $\approx \rho_0/2$. We note that the confidence regions we obtained slightly depend on the considered impact parameter interval: however, our main conclusions are stable against this arbitrary choice.

To conclude, in this work we have confronted the experimentally measured impact parameter dependence of the isospin transport ratio in ^{58,64}Ni+^{58,64}Ni collisions at 32 MeV/nucleon with the predictions of the BUU transport model using state-of-the-art effective nuclear

energy density functionals that all respect the present constraints from *ab initio* calculations. A detailed study of the time dependence of the isospin current density allows a precise determination of the density region probed by the experiment. Our analysis is in good agreement with the *ab initio* results, and produces stringent constraints on the density dependence of the symmetry energy term of the nuclear equation of state, which can be directly used for the inference of the EoS of astrophysical objects like neutron stars.

Acknowledgments We acknowledge support from Région Normandie under Réseau d'Intérêt Normand FIDNEOS (RIN/FIDNEOS). Many thanks are due to the accelerator staff of GANIL for delivering a very good quality beam and to the technical staff for the continuous support. S. Mallik acknowledges the GANIL Visiting Scientist program-2023 for very productive stay at Caen. S. Mallik also wishes to thank the VECC C&I Group for providing high-performance computational facilities.

* Electronic address: caterina.ciampi@ganil.fr
† Electronic address: swagato@vecc.gov.in

[1] C. Ciampi, J. D. Frankland, D. Gruyer, N. L. Neindre, S. Mallik, R. Bougault, A. Chbihi, L. Baldesi, S. Barlini, E. Bonnet, et al., submitted to Phys. Rev. C (2024), 2412.13648, URL https://arxiv.org/abs/2412.13648.

[2] S. Huth, P. T. H. Pang, I. Tews, T. Dietrich, A. Le Fèvre, A. Schwenk, W. Trautmann, K. Agarwal, M. Bulla, M. W. Coughlin, et al., Nature **606**, 276 (2022), URL https://www.nature.com/articles/s41586-022-04750-w.

[3] J. M. Lattimer, Annual Review of Nuclear and Particle Science **71**, 433 (2021), URL https://doi.org/10.1146/annurev-nucl-102419-124827.

[4] A. Sorensen, K. Agarwal, K. W. Brown, Z. Chajecki, P. Danielewicz, C. Drischler, S. Gandolfi, J. W. Holt, M. Kaminski, C.-M. Ko, et al., Progress in Particle and Nuclear Physics **134**, 104080 (2024), ISSN 0146-6410, URL https://www.sciencedirect.com/science/article/pii/S0146641023000613.

[5] H. Wolter, M. Colonna, D. Cozma, P. Danielewicz, C. M. Ko, R. Kumar, A. Ono, M. B. Tsang, J. Xu, Y.-X. Zhang, et al., Progress in Particle and Nuclear Physics **125**, 103962 (2022), ISSN 0146-6410, URL https://www.sciencedirect.com/science/article/pii/S0146641022000230.

[6] J. Xu, H. Wolter, M. Colonna, M. D. Cozma, P. Danielewicz, C. M. Ko, A. Ono, M. B. Tsang, Y.-X. Zhang, H.-G. Cheng, et al. (TMEP Collaboration), Phys. Rev. C **109**, 044609 (2024), URL https://link.aps.org/doi/10.1103/PhysRevC.109.044609.

[7] B.-A. Li, L.-W. Chen, and C. M. Ko, Physics Reports **464**, 113 (2008), ISSN 0370-1573, URL https://www.sciencedirect.com/science/article/pii/S0370157308001269.

[8] J. Carlson, S. Gandolfi, F. Pederiva, S. C. Pieper, R. Schiavilla, K. E. Schmidt, and R. B. Wiringa, Rev. Mod. Phys. **87**, 1067 (2015), URL https://link.aps.org/doi/10.1103/RevModPhys.87.1067.

[9] D. Adhikari, H. Albataineh, D. Androic, K. Aniol, D. S. Armstrong, T. Averett, C. Ayerbe Gayoso, S. Barcus, V. Bellini, R. S. Beminiwattha, et al. (PREX Collaboration), Phys. Rev. Lett. **126**, 172502 (2021), URL https://link.aps.org/doi/10.1103/PhysRevLett.126.172502.

[10] D. Adhikari, H. Albataineh, D. Androic, K. A. Aniol, D. S. Armstrong, T. Averett, C. Ayerbe Gayoso, S. K. Barcus, V. Bellini, R. S. Beminiwattha, et al. (CREX Collaboration), Phys. Rev. Lett. **129**, 042501 (2022), URL https://link.aps.org/doi/10.1103/PhysRevLett.129.042501.

[11] B. P. Abbott, R. Abbott, T. D. Abbott, F. Acernese, K. Ackley, C. Adams, T. Adams, P. Addesso, R. X. Adhikari, V. B. Adya, et al. (LIGO Scientific Collaboration and Virgo Collaboration), Phys. Rev. X **9**, 011001 (2019), URL https://link.aps.org/doi/10.1103/PhysRevX.9.011001.

[12] F. Rami, Y. Leifels, B. de Schauenburg, A. Gobbi, B. Hong, J. P. Alard, A. Andronic, R. Averbeck, V. Barret, Z. Basrak, et al. (FOPI Collaboration), Phys. Rev. Lett. **84**, 1120 (2000), URL https://link.aps.org/doi/10.1103/PhysRevLett.84.1120.

[13] M. B. Tsang, W. A. Friedman, C. K. Gelbke, W. G. Lynch, G. Verde, and H. S. Xu, Phys. Rev. Lett. **86**, 5023 (2001), URL https://link.aps.org/doi/10.1103/PhysRevLett.86.5023.

[14] M. B. Tsang, J. R. Stone, F. Camera, P. Danielewicz, S. Gandolfi, K. Hebeler, C. J. Horowitz, J. Lee, W. G. Lynch, Z. Kohley, et al., Phys. Rev. C **86**, 015803 (2012), URL https://link.aps.org/doi/10.1103/PhysRevC.86.015803.

[15] Y. Zhang, D. D. S. Coupland, P. Danielewicz, Z. Li, H. Liu, F. Lu, W. G. Lynch, and M. B. Tsang, Phys. Rev. C **85**, 024602 (2012), URL https://link.aps.org/doi/10.1103/PhysRevC.85.024602.

[16] C. Ciampi, S. Piantelli, G. Casini, G. Pasquali, J. Quicray, L. Baldesi, S. Barlini, B. Borderie, R. Bougault, A. Camaiani, et al., Physical Review C **106**, 024603 (2022), URL https://link.aps.org/doi/10.1103/PhysRevC.106.024603.

[17] S. Mallik, F. Gulminelli, and D. Gruyer, Journal of Physics G: Nuclear and Particle Physics **49**, 015102 (2021), URL https://dx.doi.org/10.1088/1361-6471/ac3473.

[18] R. Bougault, G. Poggi, S. Barlini, B. Borderie, G. Casini, A. Chbihi, N. Le Neindre, M. Pârlog, G. Pasquali, S. Piantelli, et al. (the FAZIA collaboration), Eur. Phys. J. A **50**, 47 (2014), URL https://doi.org/10.1140/epja/i2014-14047-4.

[19] S. Valdré, G. Casini, N. Le Neindre, M. Bini, A. Boiano, B. Borderie, P. Edelbruck, G. Poggi, F. Salomon, G. Tortone, et al., Nuclear Instruments and Methods in Physics Research Section A: Accelerators, Spectrometers, Detectors and Associated Equipment **930**, 27 (2019), URL https://linkinghub.elsevier.com/retrieve/pii/S0168900219304243.

[20] J. D. Frankland, D. Gruyer, E. Bonnet, B. Borderie, R. Bougault, A. Chbihi, J. E. Ducret, D. Durand, Q. Fable, M. Henri, et al. (INDRA Collaboration), Phys. Rev. C **104**, 034609 (2021), URL https://link.aps.org/doi/10.1103/PhysRevC.104.034609.

[21] J. Margueron, R. Hoffmann Casali, and F. Gulminelli,

Phys. Rev. C **97**, 025805 (2018), URL https://link.aps.org/doi/10.1103/PhysRevC.97.025805.

[22] V. Baran, M. Colonna, V. Greco, and M. Di Toro, Physics Reports **410**, 335 (2005), ISSN 0370-1573, URL https://www.sciencedirect.com/science/article/pii/S0370157305000025.

[23] C. Ciampi, S. Piantelli, G. Casini, A. Ono, J. D. Frankland, L. Baldesi, S. Barlini, B. Borderie, R. Bougault, A. Camaiani, et al., Physical Review C **108**, 054611 (2023), URL https://link.aps.org/doi/10.1103/PhysRevC.108.054611.

[24] S. Mallik, S. Das Gupta, and G. Chaudhuri, Phys. Rev. C **91**, 034616 (2015), URL https://link.aps.org/doi/10.1103/PhysRevC.91.034616.

[25] S. Mallik and G. Chaudhuri, Nuclear Physics A **1002**, 121948 (2020), ISSN 0375-9474, URL https://www.sciencedirect.com/science/article/pii/S037594742030258X.

[26] M. Colonna, Y.-X. Zhang, Y.-J. Wang, D. Cozma, P. Danielewicz, C. M. Ko, A. Ono, M. B. Tsang, R. Wang, H. Wolter, et al., Phys. Rev. C **104**, 024603 (2021), URL https://link.aps.org/doi/10.1103/PhysRevC.104.024603.

[27] Y.-X. Zhang, Y.-J. Wang, M. Colonna, P. Danielewicz, A. Ono, M. B. Tsang, H. Wolter, J. Xu, L.-W. Chen, D. Cozma, et al., Phys. Rev. C **97**, 034625 (2018), URL https://link.aps.org/doi/10.1103/PhysRevC.97.034625.

[28] S. J. Lee, H. H. Gan, E. D. Cooper, and S. Das Gupta, Phys. Rev. C **40**, 2585 (1989), URL https://link.aps.org/doi/10.1103/PhysRevC.40.2585.

[29] W. D. Myers, Nuclear Physics A **296**, 177 (1978), ISSN 0375-9474, URL https://www.sciencedirect.com/science/article/pii/0375947478904207.

[30] C. Drischler, K. Hebeler, and A. Schwenk, Phys. Rev. C **93**, 054314 (2016), URL https://link.aps.org/doi/10.1103/PhysRevC.93.054314.

[31] G. A. Lalazissis, J. König, and P. Ring, Phys. Rev. C **55**, 540 (1997), URL https://link.aps.org/doi/10.1103/PhysRevC.55.540.

[32] N. Van Giai and H. Sagawa, Physics Letters B **106**, 379 (1981), ISSN 0370-2693, URL https://www.sciencedirect.com/science/article/pii/0370269381906468.

[33] B. T. Reed, F. J. Fattoyev, C. J. Horowitz, and J. Piekarewicz, Phys. Rev. C **109**, 035803 (2024), URL https://link.aps.org/doi/10.1103/PhysRevC.109.035803.

[34] Z. Xiao, B.-A. Li, L.-W. Chen, G.-C. Yong, and M. Zhang, Phys. Rev. Lett. **102**, 062502 (2009), URL https://link.aps.org/doi/10.1103/PhysRevLett.102.062502.

[35] X. Roca-Maza, G. Colò, and H. Sagawa, Phys. Rev. C **86**, 031306 (2012), URL https://link.aps.org/doi/10.1103/PhysRevC.86.031306.

[36] R. J. Lenk and V. R. Pandharipande, Phys. Rev. C **39**, 2242 (1989), URL https://link.aps.org/doi/10.1103/PhysRevC.39.2242.

[37] S. Mallik, G. Chaudhuri, and F. Gulminelli, Phys. Rev. C **100**, 024611 (2019), URL https://link.aps.org/doi/10.1103/PhysRevC.100.024611.

[38] A. Camaiani, S. Piantelli, A. Ono, G. Casini, B. Borderie, R. Bougault, C. Ciampi, J. A. Dueñas, C. Frosin, J. D. Frankland, et al., Physical Review C **102**, 044607 (2020), URL https://doi.org/10.1103/PhysRevC.102.044607https://link.aps.org/doi/10.1103/PhysRevC.102.044607.

[39] S. Huth, C. Wellenhofer, and A. Schwenk, Phys. Rev. C **103**, 025803 (2021), URL https://link.aps.org/doi/10.1103/PhysRevC.103.025803.